



This is a repository copy of *Combining PTH(1-34) and mechanical loading has increased benefit to tibia bone mechanics in ovariectomised mice*.

White Rose Research Online URL for this paper:

<https://eprints.whiterose.ac.uk/208086/>

Version: Published Version

---

**Article:**

Roberts, B.C., Cheong, V.S., Oliviero, S. et al. (4 more authors) (2024) Combining PTH(1-34) and mechanical loading has increased benefit to tibia bone mechanics in ovariectomised mice. *Journal of Orthopaedic Research*, 42 (6). pp. 1254-1266. ISSN 0736-0266

<https://doi.org/10.1002/jor.25777>

---

**Reuse**

This article is distributed under the terms of the Creative Commons Attribution (CC BY) licence. This licence allows you to distribute, remix, tweak, and build upon the work, even commercially, as long as you credit the authors for the original work. More information and the full terms of the licence here:

<https://creativecommons.org/licenses/>

**Takedown**


If you consider content in White Rose Research Online to be in breach of UK law, please notify us by emailing [eprints@whiterose.ac.uk](mailto:eprints@whiterose.ac.uk) including the URL of the record and the reason for the withdrawal request.



[eprints@whiterose.ac.uk](mailto:eprints@whiterose.ac.uk)  
<https://eprints.whiterose.ac.uk/>

## RESEARCH ARTICLE

# Combining PTH(1-34) and mechanical loading has increased benefit to tibia bone mechanics in ovariectomised mice

Bryant C. Roberts<sup>1,2,3</sup> | Vee San Cheong<sup>2,4</sup> | Sara Oliviero<sup>1,2</sup> |  
Hector M. Arredondo Carrera<sup>1</sup> | Ning Wang<sup>1</sup> | Alison Gartland<sup>1</sup> | Enrico Dall'Ara<sup>1,2</sup> 

<sup>1</sup>Division of Clinical Medicine, University of Sheffield, Sheffield, UK

<sup>2</sup>Insigneo Institute for in silico Medicine, University of Sheffield, Sheffield, UK

<sup>3</sup>Adelaide Microscopy, Division of Research and Innovation, The University of Adelaide, Adelaide, South Australia, Australia

<sup>4</sup>Department of Automatic Control and Systems Engineering, University of Sheffield, Sheffield, UK

## Correspondence

Enrico Dall'Ara, Insigneo Institute for in silico Medicine, University of Sheffield, Pam Liversidge Bldg, Sheffield S1 3JD, UK.  
Email: [e.dallara@sheffield.ac.uk](mailto:e.dallara@sheffield.ac.uk)

## Funding information

Engineering and Physical Sciences Research Council, Grant/Award Numbers: EP/K03877X/1, EP/S032940/1; National Centre for the Replacement Refinement and Reduction of Animals in Research, Grant/Award Number: NC/R001073/1

## Abstract

Combined treatment with PTH(1-34) and mechanical loading confers increased structural benefits to bone than monotherapies. However, it remains unclear how this longitudinal adaptation affects the bone mechanics. This study quantified the individual and combined longitudinal effects of PTH(1-34) and mechanical loading on the bone stiffness and strength evaluated in vivo with validated micro-finite element (microFE) models. C57BL/6 mice were ovariectomised at 14-week-old and treated either with injections of PTH(1-34), compressive tibia loading or both interventions concurrently. Right tibiae were in vivo microCT-scanned every 2 weeks from 14 until 24-week-old. MicroCT images were rigidly registered to reference tibia and the cortical organ level (whole bone) and tissue level (midshaft) morphometric properties and bone mineral content were quantified. MicroCT images were converted into voxel-based homogeneous, linear elastic microFE models to estimate the bone stiffness and strength. This approach allowed us for the first time to quantify the longitudinal changes in mechanical properties induced by combined treatments in a model of accelerated bone resorption. Both changes of stiffness and strength were higher with co-treatment than with individual therapies, consistent with increased benefits with the tibia bone mineral content and cortical area, properties strongly associated with the tibia mechanics. The longitudinal data shows that the two bone anabolics, both individually and combined, had persistent benefit on estimated mechanical properties, and that benefits (increased stiffness and strength) remained after treatment was withdrawn.

## KEYWORDS

in vivo microCT, mechanical properties, ovariectomy, parathyroid hormone, tibia loading

## 1 | INTRODUCTION

Osteoporosis (OP) reduces the bone mineral density, decreases the bone strength, and increases the risk of fracture, in women and men<sup>1</sup>. It is a major clinical<sup>1</sup> problem for the ageing society and affects one in

three women and one in five men above 50-year-old.<sup>2</sup> Reduced fracture risk is the ultimate goal in any treatment for OP.<sup>3</sup> Currently, there exist many pharmacological treatments for OP found to be effective at improving the bone mass and structural properties, at increasing the bone strength<sup>4,5</sup> and reducing the fracture prevalence.<sup>6</sup>

This is an open access article under the terms of the [Creative Commons Attribution](https://creativecommons.org/licenses/by/4.0/) License, which permits use, distribution and reproduction in any medium, provided the original work is properly cited.

© 2023 The Authors. *Journal of Orthopaedic Research*® published by Wiley Periodicals LLC on behalf of Orthopaedic Research Society.

Current OP interventions include pharmacological treatments based on bone anabolics (e.g., injections of Parathyroid Hormone PTH, as the FDA approved Teriparatide), antiresorptives (bisphosphonates), or antibody targeting sclerostin.<sup>7</sup> While these therapies are most effective at reducing vertebral fractures, the treatment benefits to hip and other nonvertebral sites are less pronounced.<sup>8,9</sup> PTH(1-34) is a bone anabolic shown to strengthen the skeleton by promoting bone osteogenesis, and further to increase the cortical bone response to mechanical stimuli.<sup>10</sup> Pretreatment with PTH thus has the benefit of mitigating an inherent risk of mechanical loading; inducing the very fracture it is meant to prevent. However, teriparatide is only approved by the US Food and Drug Administration for use in patients with severe osteoporosis up to a maximum of 2 years.<sup>11</sup> Investigating the interaction of mechanical loading and PTH on the bone properties is helpful to develop novel treatments and strategies that reduce fracture likelihood and the associated personal and societal costs.

Preclinical studies in mice are useful for the rapid testing of these treatment regimens,<sup>12</sup> with the ovariectomy model being the most used rodent model to test new treatments for OP. Longitudinally, studies on antiosteoporotic therapies will often measure the effect of treatments only on the microstructural properties of the trabecular bone (e.g., trabecular bone volume fraction and thickness) or the cortical bone (e.g., cortical bone area).<sup>13-16</sup> Previous studies have found that ovariectomy (OVX) reduces the amount of trabecular bone (reduced bone volume fraction, increased spacing, decreased number) in the proximal mouse tibia, whereas little effects were found in the cortical bone in its midshaft, and that these findings are mouse strain dependent.<sup>17</sup> In particular, it was found that ovariectomy has a larger effect on the densitometric properties of the tibia cortical bone in C57BL/6 mice than in BALB/C mice and that effects on cortical thickness could be observed only after 4 weeks from OVX and only for the C57BL/6 mice.<sup>18</sup> However, the bone mechanical properties, in particular the bone strength, are recommended as more clinically relevant endpoints.<sup>19</sup> While bone mechanical properties have been assessed through standard mechanical testing (e.g., three-/four-point bending),<sup>20</sup> the destructive nature of these tests prohibits monitoring of biomechanical changes in a single animal over time, and thus are limited to studies of cross-sectional design. Sometimes, where mechanical tests are not performed, the change in the murine tibia structure, derived using *in vivo* micro-computed tomography (microCT) imaging and recommended in a small mid-shaft region of interest,<sup>21</sup> is considered as surrogate of change in the bone's mechanical properties.<sup>22</sup> However, little is known about the relationships between the mouse tibia mechanical and structural properties in compressive loading. Understanding these relationships is fundamental to understand to what extent (i.e., under what loading conditions) we can reasonably use these surrogate measurements. Computational models based on *in vivo* microCT images have the potential of assessing *in vivo* the biomechanical properties of bones. Nevertheless, these models have to be comprehensively validated against experiments in the laboratory before their application *in vivo*. Recently, we have shown that microCT-based micro-finite element (microFE) models of the mouse tibia can be used to evaluate accurately the bone stiffness, bone strength and local deformation, as compared

against state of the art biomechanical experiments.<sup>23,24</sup> These models are useful to noninvasively evaluate the longitudinal mechanical behavior of the mouse bone.<sup>18,25</sup>

PTH and compressive mechanical loading, both individually and combined, have proven benefits to the appendicular bone structure of ovariectomised mice.<sup>16,26</sup> While PTH(1-34) requires a "bone anabolic window" to induce an effective osteogenic response, little is known about its combination with mechanical loading. We have previously shown that these treatments induce heterogeneous morphometric and densitometric changes across the length of the mouse tibia in an OVX mouse model. In particular, our findings revealed highly-region dependent adaptations, with an increased benefit from combined treatment with loading and PTH to the posterior-lateral region of the mid-diaphyseal bone.<sup>16</sup> Recently, a cross-sectional study on C57BL/6 (not OVX) mice showed that the bone anabolic response to a combination of mechanical loading and PTH depends on the dose and regimen of the intervention and that it affects differently the trabecular and cortical compartments, highlighting the potential of the combined biomechanical and pharmacological treatment.<sup>27</sup> Nevertheless, in those studies it was not investigated how the bone anabolic effects would affect the mechanical properties of the bone at early or later stages of treatments. To our knowledge, no study has evaluated yet the combined longitudinal effects of PTH and loading on tibia bone mechanics in an ovariectomised mouse model of OP.

The aim of this study was to quantify the individual and combined effects of PTH(1-34) and a controlled, externally applied load, on the tibia stiffness and strength (failure load) in an ovariectomised mouse model of osteoporosis. Given strong associations between tibia bone mineral content and the bone stiffness and strength reported elsewhere,<sup>25</sup> we hypothesize that combining treatments will further improve the mechanical properties beyond the therapeutic benefits of individual treatments alone. A secondary aim was to evaluate organ level and tissue level structural determinants of the bone mechanical properties to confirm potential of surrogate measurements for the bone mechanical properties.

## 2 | METHODS

### 2.1 | Animals and study design

Eighteen female virgin C57BL/6 mice (Charles River UK Ltd.), and as described elsewhere,<sup>16</sup> were housed in the University of Sheffield's Biological Services Unit from 13-week-old: four mice per cage at 22°C, with a 12-h dark/light cycle and *ad libitum* access to 2918 Teklad Global 18% protein rodent diet (Envigo RMS Ltd.) and water. All the procedures were performed under a British Home Office licence (PF61050A3) and in compliance with the Animal (Scientific Procedures) Act 1986. This study was reviewed and approved by the local Research Ethics Committee of The University of Sheffield. The findings and experiments in this paper were designed and reported in accordance with the ARRIVE guidelines.

C57BL/6 mice were chosen due to documented skeletal responsiveness to mechanical loading, PTH(1-34) or OVX.<sup>10,16,18,25</sup> These mice were considered to be skeletally mature at the onset of this study, given that peak cortical bone mass was elsewhere documented in this mouse strain between 3 and 4 months of age.<sup>28</sup> An a priori estimate of sample size was computed based on large loading effects to cortical thickness after 6 weeks of loading in PTH-treated mice,<sup>22</sup> indicating that six mice per group was necessary to achieve 80% statistical power and assuming Cohen's  $d = 2$ ,  $\alpha = 0.05$ .

At 14-week-old, mice underwent OVX and remained untreated for 4 weeks following surgery to allow OVX-induced bone adaptation.<sup>18</sup> The OVX group was chosen as control as it is widely accepted as mouse model for OP and requested by the regulatory bodies when testing new treatments preclinically. Mice were randomized, one mouse from each cage, into three treatment groups ( $n = 6$  mice/group) and then treated on Weeks 18–22, and per schedule in Figure 1, with either (1) PTH(1-34), “PTH” group, (2) mechanical loading, “ML” group, (3) concurrent treatment with PTH(1-34) and mechanical loading, “ML+PTH” group. All mice were withdrawn from treatment for the final 2 weeks of the study (Weeks 23 and 24). Treatment effects were confirmed by comparing bone structural and mechanical properties with a comparator group ( $n = 5$ ), age-matched female C57BL/6 mice that were ovariectomized at 14-week-old and received no treatment: “OVX” group.<sup>18</sup>

All analyses in this study were performed on the right tibia of each mouse. The measurements obtained at the time of treatment onset (18-week-old) provided internal control for each mouse.

## 2.2 | Intraperitoneal PTH(1-34) injections

Between Weeks 18 and 22 inclusive, mice received either intraperitoneal injection of PTH(1-34) (Bachem) at 100  $\mu\text{g}/\text{kg}/\text{day}$ , 5 days/week on Monday to Friday (groups: PTH, ML+PTH) or vehicle (group: ML). PTH

was prepared in 1% acetic acid and 2% heat inactivated mouse serum in Hanks' Balanced Saline Solution.<sup>25</sup> We chose the dose of 100  $\mu\text{g}/\text{kg}/\text{day}$  based on our preliminary experiments in nonoperated mice<sup>25</sup> and previous studies that have shown optimal benefits.<sup>29,30</sup>

## 2.3 | Mechanical loading

In ML and ML+PTH groups, the right tibia was uniaxially compressed along the superior–inferior axis to a peak load of 12.0 N by superimposing a dynamic load of 10.0 N upon a static 2.0 N preload. Forty trapezoidal waveform load cycles were applied (held for 0.2 s at 12.0 N) with a 10 s interval between each cycle. Tibia loading was applied for six individual sessions, 3 days per week (Monday, Wednesday, Friday), during Weeks 19 and 21 of age. A 12 N load was chosen as this was previously shown to confer significant bone apposition in female C57BL/6 mice without impairing mobility following treatment.<sup>31</sup> This load we have shown from microFE estimates and experimentally to engender peak strain between  $-2330$  and  $-4825$  microstrain among OVX and control mice,<sup>32</sup> though the strain can be affected by alignment during in vivo loading expected to occur intraexperimentally.<sup>33</sup> Ten-second rest interval was shown to enhance osteogenic effects of loading.<sup>34</sup> Very few load cycles (as low as 40 tibia compressions) and over few days has been recommended<sup>35</sup> and shown reliably to induce bone formation.<sup>22,36</sup> Further, increasing the number of loading cycles by order of magnitude does not enhance bone formation response.<sup>37</sup>

## 2.4 | In vivo microCT imaging and analysis

For each mouse, only the whole right tibia was in vivo microCT scanned (VivaCT80; Scanco Medical). Mice were positioned in the microCT scanner on the scanning bed with animal holder provided by

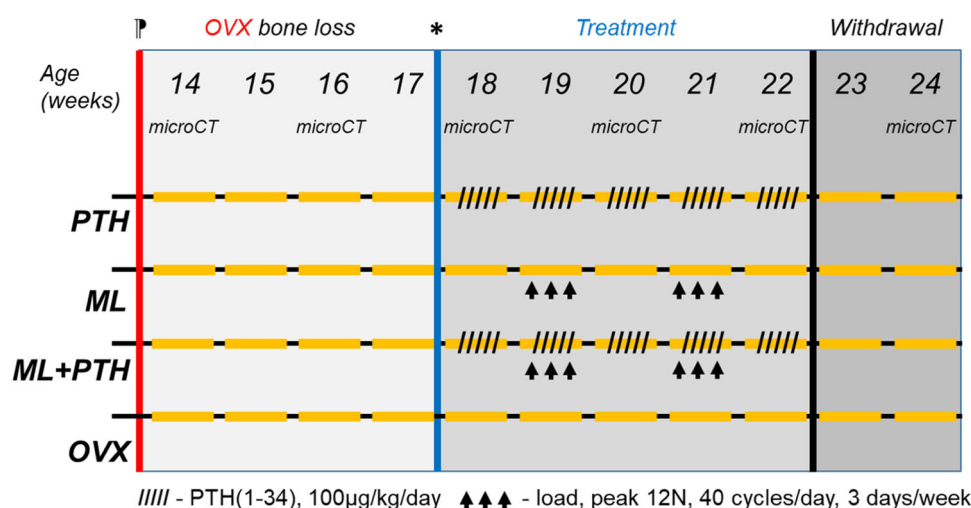


**FIGURE 1** Study design and treatment schedule in C57BL/6 female mice. Ovariectomy (OVX) was performed at 14-week-old; \*treatment commenced at 18 weeks and was withdrawn at 22 weeks of age. Treatment groups ( $n = 6$  mice/group) PTH: PTH(1-34) only; ML: mechanical loading only; ML+PTH: PTH(1-34) and mechanical loading. This figure was amended with permission from Roberts et al.<sup>16</sup> OVX mice were reported and described in detail previously in Roberts et al.<sup>18</sup> [Color figure can be viewed at [wileyonlinelibrary.com](https://onlinelibrary.wiley.com/doi/10.1002/jor.25777)]

the manufacturer that allowed to have a single leg in the field of view. A baseline scan (before OVX surgery) was performed at 14-week-old, then follow-up in vivo scans were performed every 2 weeks until Week 22 (Figure 1). At Week 24, mice were euthanized by cervical dislocation and the right tibia microCT-scanned ex vivo per the in vivo imaging protocol. The following scanning parameters, optimized in a previous study,<sup>38</sup> were applied: 10.4  $\mu\text{m}$  isotropic voxel size, voltage of 55 kVp, intensity of 145  $\mu\text{A}$ , field of view of 32 mm, 750 projections/180°, integration time 100 ms and 0.5 mm Al Filter. This scanning protocol induced 256 mGy dose to the mouse limb. In ovariectomized C57BL/6 mice, we found that repeated scans with this protocol reduced trabecular bone volume, attributed to fewer trabeculae. However, repeated scans had minimal effects on the remaining bone structures and did not affect mechanical properties evaluated in this study, which are less affected by changes in metaphyseal trabecular morphometry.<sup>39</sup> A third-order polynomial beam hardening correction algorithm based on a 1200 mg HA/cm<sup>3</sup> wedge phantom was applied to all the scans.<sup>40</sup> A calibration law based on weekly quality checks performed on a five-rod densitometric phantom was used to convert Hounsfield Units in each image into tissue mineral density (TMD) equivalent values. The reconstructed microCT images were exported from the microCT evaluation software as DICOM files for further processing.

## 2.5 | Image alignment and preprocessing

Before image and finite-element analysis, a rigid registration procedure was applied to all scans so that tibiae specimens were, regardless of different orientations in the microCT scanner, aligned to a common reference system. Image registration significantly improves the precision of structural measurements in longitudinal in vivo microCT studies,<sup>41</sup> and ensures consistent alignment of bone along the longitudinal axis for evaluating bone mechanics with finite-element analysis. One tibia at Week 14 of age was used as the reference specimen of which the longitudinal axis was approximately aligned with the z-axis of the global reference system. Each image of remaining tibia at 14-week-old was then rigidly registered to the reference tibia, and the tibia of each mouse at remaining time-points (Weeks 16–24) subsequently registered to the 14-week-old reference specimen. Rigid registration was performed on the greyscale images in software Amira (v5.4.3; FEI Visualization Sciences Group) using a Quasi-Newton optimizer and Normalized Mutual Information as the similarity measure. A Gaussian filter (kernel  $3 \times 3 \times 3$ , standard deviation 0.65) was applied to all registered images to reduce high frequency noise and images were binarised using a global threshold that was specific to each mouse and defined as the average of the gray levels between bone and background peaks in each image histogram.<sup>38,42</sup> Specimen-specific thresholding has been recommended for cases where bone mineralization could differ among the study groups.<sup>21</sup> Further, at 10  $\mu\text{m}$  pixel size good agreement was observed between the above histogram-based thresholding method and operator-based thresholding for quantifying trabecular

properties,<sup>42</sup> which can be an order of magnitude thinner than the cortical bone that was the focus herein. We have shown that using a fixed threshold across all specimens leads to higher or comparable errors than using specimen-specific thresholding, in trabecular morphometry when compared with higher resolution ex vivo microCT scans (4  $\mu\text{m}$  pixel size; see supplementary materials in Oliviero et al.<sup>38</sup>).

Across all time points and mice, the mean ( $\pm$  Standard Deviation, SD) tibia metaphyseal trabecular thickness and midshaft cortical thickness were  $52 \pm 9 \mu\text{m}$  and  $238 \pm 30 \mu\text{m}$ , respectively. With the 10.4  $\mu\text{m}$  pixel size used herein, smaller individual trabeculae were 3–6 pixel in width. This resolution was found to provide good agreement with most trabecular properties measured in higher resolution scans (4–6  $\mu\text{m}$  voxel size), as shown by our laboratory<sup>38,43</sup> and others.<sup>42</sup>

## 2.6 | Morphometric and densitometric analysis

The tibia length (L) was measured at each time point, and a volume equal in height to 80% of the tibia length was cropped starting immediately below the proximal growth plate (as shown in Figure 2). By selecting the 80% length we remove the growth plates and primary trabecular close to them that increased the densitometric measurement errors,<sup>44</sup> and furthermore focus the analysis on systemic bone adaptations that are a feature of OP (e.g., secondary trabecular bone loss<sup>18</sup> or gain<sup>16</sup> due to hormonal and pharmacological interventions) compared with local adaptation that occur in the bone epiphyses and may be affected by physiological loading (i.e., due to daily cage activity). This method removes ~6% of the proximal tibia. While extending the region closer to the growth plate may improve sensitivity to detect bone changes as shown elsewhere,<sup>45</sup> it was not considered in the current study considering the measurement errors and that the trabecular region has minimal impact on bone mechanics estimates. Removal of the distal growth-plate was confirmed by visual inspection in all specimens. In the 80%L volume of interest (VOI), cortical bone structural properties were computed using custom scripts (MatLab 2018a; The Mathworks Inc.), including: bone mineral content (BMC), tissue mineral density (TMD), bone volume (BV), and cortical area (Ct.Ar80%L, mm<sup>2</sup>) which was defined as the bone volume (BV, mm<sup>3</sup>) divided by 80% of L (mm). Averaging cross-sectional area over the 80%L VOI allows comparison across time points as the tibia continues to lengthen and affects the BV measurement.<sup>14</sup> Tibia length varied among mice between 16.93 and 18.82 mm (corresponding with 80%L: 13.54–15.05 mm). BMC was computed by multiplying the voxel size by the sum of the TMD values over the total bone volume within each VOI. The polar moment of inertia (J) and cortical thickness (Ct.Th) and area (Ct.Ar mid) were computed in a 1 mm thick region in the cortical midshaft (centered along 50% of L). Engineering theory dictates that Ct.Ar is the most relevant morphological parameter to compressive mechanical tests.<sup>20</sup> We analyzed the midshaft structural properties, consistent with guidelines defined in Jepsen et al.<sup>20</sup> which is the region of bone most commonly investigated via microCT. However, treatments can affect



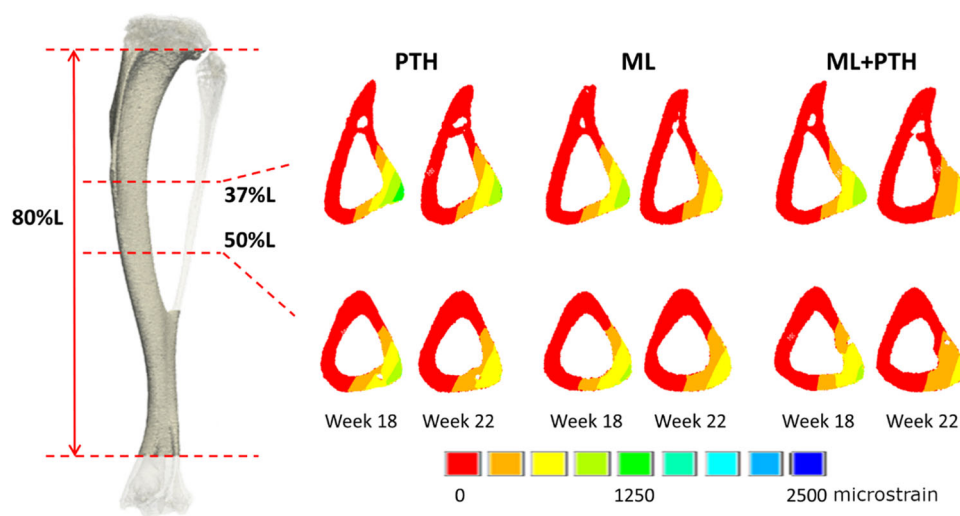


**FIGURE 2** Third principal strain distribution in tibia cross-sections at 37% and 50% of the bone length (relative to proximal end) in representative specimen from each treatment group and at treatment onset (Week 18) and treatment withdrawal (Week 22). [Color figure can be viewed at [wileyonlinelibrary.com](https://onlinelibrary.wiley.com/doi/10.1002/jor.25777)]

differently regions of bone, considering the highly variable cross-sectional morphology of mice bone along its longitudinal axis,<sup>46</sup> thus the whole modeled region of interest (80%L) was examined. All properties were quantified using CT analyser (v1.20.3.0; Skyscan-Bruker).

## 2.7 | Micro-finite element analysis

Subject-specific microFE models of each tibia at each time point were generated from the 80%L VOI. All models excluded the fibula (Figure 2). A connectivity filter (connectivity rule = 6, bwlabeln function in Matlab) was used to remove from the binary image the unconnected bone islands and the connected bone voxels were converted into 8-node hexahedral elements. Bone was considered homogenous, isotropic, and linear elastic, with a modulus of elasticity of 14.8 GPa, and Poisson's ratio of 0.3.<sup>23,32</sup> Uniaxial compression was applied by fixing the nodes of the most distal section of the model and by applying an axial displacement equal to 0.1 mm at the proximal end. The structural apparent stiffness was calculated as the measured reaction force in the longitudinal direction divided by the applied displacement. The failure load was estimated from the linear microFE models as the amount of force required for 10% of the nodes to reach the yield strain (third principal strain of  $-14,420$  microstrains).<sup>24</sup> The 10% of the model was excluded from this analysis at each extremity to reduce the effect of the application of the boundary conditions at the most proximal and most distal slices of the modeled portion of the tibia. These models have been recently validated against state-of-the-art experiments for the prediction of local deformation and structural properties.<sup>23,32</sup> The resulting linear microFE models were solved (Ansys, Release 15.0, ANSYS, Inc.) on a high-performance computing (HPC) system (ShARC, University of Sheffield; 8 cores, memory = 32GB/core) in approximately 30 min. MicroFE models were recently validated against experiments

with mean error of  $14 \pm 8\%$  and  $9 \pm 6\%$  for the stiffness and strength estimates, respectively.<sup>24</sup>

## 2.8 | Statistics

Data were analyzed by two-way mixed Analysis of Variance (ANOVA). Where for a given bone property the *F*-values were significant for a "time-by-intervention" interaction, the simple "time-effect" was investigated using paired *t*-tests between (1) treatment baseline (Week 18) and proceeding time-points (Weeks 20–24) and (2) between sequential time-points (i.e., Weeks 20–24 comparisons).<sup>13,18</sup> Between group differences in bone properties due to treatment and treatment withdrawal (i.e., at Weeks 20, 22, and 24) were analyzed using Analysis of Covariance (ANCOVA), adjusted for values at 18-week-old and with post hoc Bonferroni-adjusted pairwise comparisons. Adjustment for Week 18 values mitigates biases due to potential group differences in the bone properties at the onset of treatment. Herein, structural properties differed between ML and ML+PTH mice at Week 18 (Supporting Information S1: Table 1 and Figure 3). Finally, linear regression analyses were performed to evaluate relationships between the structural properties (morphometric, densitometric) of the tibia and its estimated mechanical properties. Regression analysis was used to determine the ability of organ- and tissue-level structural properties (e.g., BMC, Ct.Ar<sub>80%L</sub>, Ct.Ar<sub>mid</sub>) to predict microFE estimates of the bone stiffness and strength. The differences between the  $R^2$  values of organ and tissue-level regressions for predicting bone mechanics were assessed using Steiger's *Z* test for dependent samples.<sup>47</sup> The structural properties were then forward entered into multivariable linear regression to assess whether additional properties could improve the prediction of the tibia mechanics. Statistical significance was set at  $\alpha = 0.05$ . All analyses were performed using SPSS Statistics<sup>25</sup> (IBM Corp.).

### 3 | RESULTS

All treated mice completed this study without complication, for example, there were no observable impairments in the limb following mechanical loading that could otherwise affect the mouse gait and bone adaptations. Uterine mass at the end of this study was significantly lower in the OVX group than in nonoperated controls as we previously reported<sup>18</sup> (uterine mass:  $8.6 \pm 2.4$  mg vs.  $83.5 \pm 15.4$  mg,  $p < 0.001$ ).

#### 3.1 | Longitudinal effects of PTH(1-34) and mechanical loading on the bone length, bone morphometric, and the estimated mechanical properties

No woven bone formation was observed among study groups (Supporting Information S1: Figure 1, nor an increase in the tibia cortical porosity, both of which have been reported elsewhere and may be a consequence of longer PTH administration<sup>10</sup> or a combination of PTH and higher applied external loads<sup>22</sup> than in this paper.

Significant "time-by-intervention" interaction and "time-effect" were observed for bone size, morphometric properties and estimated

mechanical properties. In all treatment groups, a significant and persistent increase in the tibiaBMC and Ct.Ar<sub>80%L</sub> was observed from Weeks 18–20 to 20–22 (Figure 3 and Supporting Information S1: Figure 1 and Table 1,  $p < 0.005$ ). Anabolic benefits were retained following treatment withdrawal (Weeks 18–24 comparison), though Ct.Ar<sub>80%L</sub> significantly decreased from Weeks 22–24 in ML mice ( $p = 0.040$ ). In all treatment groups a persistent increase in L was observed from Weeks 18 to 22; and in OVX mice L was significantly longer at Weeks 22 and 24 than Week 18. Changes in L among all groups were relatively modest (between 1.2% and 2.3% change from Week 18 to 24,  $p < 0.01$ ; and Supporting Information S1: Figure 2).

In all groups, estimated stiffness and failure load significantly increased from Weeks 18 to 20. From weeks 20 to 22, stiffness significantly increased in ML mice, and failure load increased in ML and ML+PTH groups (Figure 3, all  $p < 0.05$ ). With the increase in tibia stiffness a decline in induced strains under the applied load was observable from Weeks 18 to 22 (Figure 2). The strain distribution, concentrating compressive strain in the posterior-lateral aspect of the tibia, was consistent with strain maps reported from microFE analysis of others who included the fibula in their model.<sup>48</sup> No significant changes in stiffness nor failure load were observed following treatment withdrawal. Individual trends for both structural and estimated mechanical properties are reported in the Supporting Information S1: Figure 3.

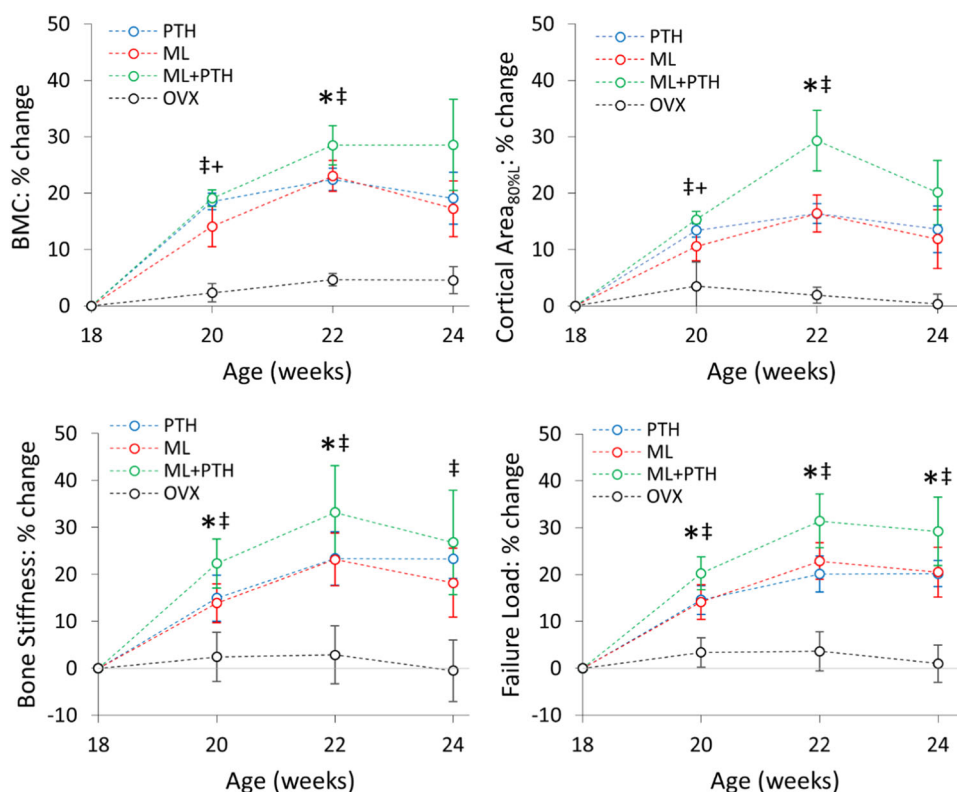


**FIGURE 3** Mean percent change ( $\pm 1$  SD), relative to Week 18 values, in (top) tibia BMC and cortical area, and (bottom) estimated stiffness and failure load. Statistically significant difference between treatment groups (ANCOVA, adjusted for Week 18 values): +PTH versus ML; \*ML+PTH versus PTH; †ML+PTH versus ML. Structural and mechanical properties were higher in all treatment groups than OVX at all time points. Readers should refer to Supporting Information S1: Figure 1 for changes in mean values for the duration of the study (including OVX effects during the pretreatment period, from Weeks 14 to 18 weeks of age). [Color figure can be viewed at [wileyonlinelibrary.com](https://onlinelibrary.wiley.com/doi/10.1002/jor.25777)]

### 3.2 | Between group differences in structural and estimated mechanical properties over time

In all treatment groups, bone properties were significantly improved compared with the OVX controls. Following adjustment for Week 18 values, both the structural and estimated mechanical properties differed among treatment groups (Figure 3). At Week 20 BMC and Ct.Ar<sub>80%L</sub> were significantly higher in PTH (percentage difference [range (95% CI)]: BMC + 4.9 (0.9, 8.9) %; Ct.Ar<sub>80%L</sub> + 3.3 (0.1, 6.4) %, all  $p < 0.05$ ) and in ML+PTH (BMC + 6.1 (1.2, 11.0) %; Ct.Ar<sub>80%L</sub> + 5.8 (1.9, 9.7) %, all  $p < 0.01$ ) than ML mice. At Week 22, BMC and Ct.Ar<sub>80%L</sub> were significantly higher in ML+PTH than PTH (BMC + 6.9 (1.9, 11.8) %; Ct.Ar<sub>80%L</sub> + 13.9 (7.0, 20.7) %, all  $p < 0.01$ ) and ML mice (BMC + 6.9 (1.0, 12.7) %; Ct.Ar<sub>80%L</sub> + 14.4 (5.7, 22.9) %, all  $p < 0.01$ ).

In ML+PTH, bone stiffness was significantly higher than in PTH at Week 20 (+10.8 (3.8, 17.9) %,  $p = 0.001$ ) and Week 22 (+12.8 (1.5, 24.2) %,  $p = 0.020$ ) and in ML mice at Weeks 20–24 (11.7–13.2 (0.2, 24.6) %,  $p < 0.05$ ). Failure load was significantly higher in ML+PTH than PTH and ML at all time points (mean difference 8.0–13.6 (1.5, 21.6) %,  $p < 0.01$ ). Neither stiffness nor the failure load differed between PTH and ML mice.

At Week 22, tibia length was significantly higher in ML+PTH than PTH groups and, at Week 24, significantly higher in loaded

limbs (ML+PTH and ML) than OVX and PTH groups ( $p < 0.05$ ) (Supporting Information S1: Figure 2).

### 3.3 | Determinants of bone estimated mechanical properties

In all treatment groups, the tibia BMC and Ct.Ar<sub>80%L</sub> were strong predictors of the bone stiffness ( $R^2$ -range: 0.769–0.904, all  $p < 0.001$ ; Figures 4 and 5) and of the failure load ( $R^2$ -range: 0.855–0.950, all  $p < 0.001$ ). The tibia length was a significant, albeit relatively weak predictor of stiffness ( $R^2$ -range: 0.253–0.700,  $p < 0.01$ ) and strength ( $R^2$ -range: 0.435–0.741,  $p < 0.01$ ). Similarly, midshaft structural properties—polar moment, cortical area and thickness—were strong predictors of the bone stiffness ( $R^2$ -range: 0.724–0.902, all  $p < 0.001$ ) and the failure load ( $R^2$ -range: 0.823–0.958, all  $p < 0.001$ ) (Figures 4 and 5). In PTH, the Ct.Ar<sub>80%L</sub> better predicted strength than Ct.Ar<sub>mid</sub> ( $R^2$ : 0.925 vs. 0.823,  $p < 0.05$ ). In ML, BMC was a better predictor of both stiffness and strength than Ct.Ar<sub>mid</sub> ( $R^2$ : 0.904 vs. 0.828, 0.936 vs. 0.852, respectively,  $p < 0.05$ ). In ML+PTH, Ct.Ar<sub>mid</sub> and polar moment better predicted strength than Ct.Ar<sub>80%L</sub> ( $R^2$ : 0.958, 0.954, and 0.855, respectively, all  $p < 0.05$ ). In the multivariable regression analysis, additional structural properties provided significant, albeit

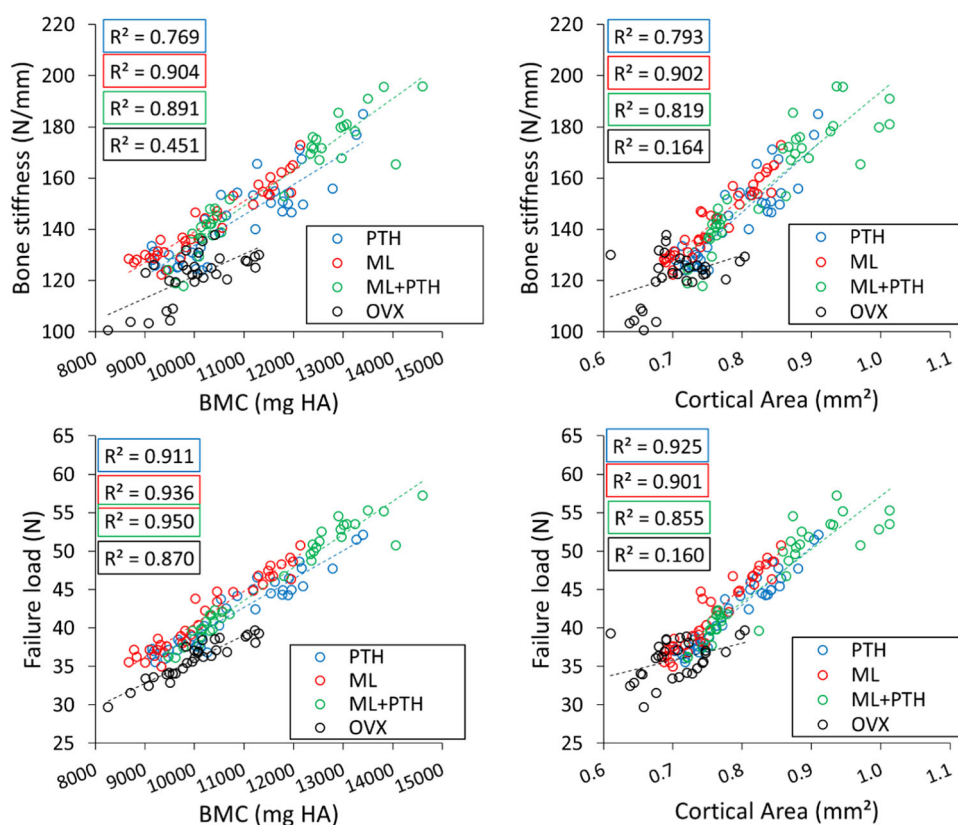


**FIGURE 4** Linear regression analyses showing for each treatment group interrelationships between the tibia structural properties and estimate stiffness (top row) or estimated failure load (bottom row). [Color figure can be viewed at [wileyonlinelibrary.com](https://onlinelibrary.wiley.com/doi/10.1002/jor.25777)]



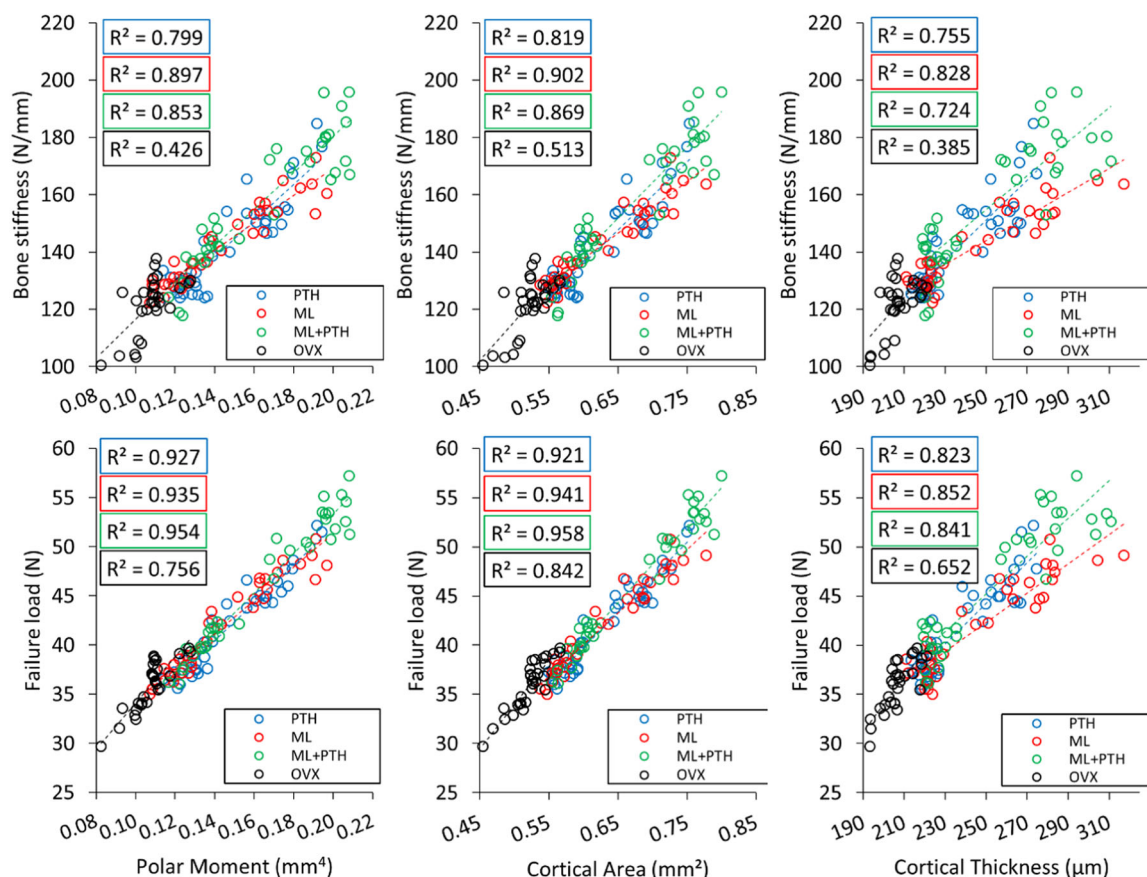


**FIGURE 5** Linear regression analyses showing for each treatment group interrelationships between the tibia midshaft structural properties and estimated stiffness (top row) or estimated failure load (bottom row). [Color figure can be viewed at [wileyonlinelibrary.com](http://wileyonlinelibrary.com)]

**TABLE 1** Summary of multiple linear regression analysis for the prediction of bone stiffness and strength.

Dependent var.	Model	R <sup>2</sup>	Adj. R <sup>2</sup>	R <sup>2</sup> change <sup>a</sup>	p Value
<b>Strength</b>					
OVX	BMC	0.870	0.865		<0.001
ML	Ct.Ar <sub>mid</sub>	0.941	0.939		<0.001
	Ct.Ar <sub>mid</sub> , BMC	0.963	0.960	0.022	<0.001
	Ct.Ar <sub>mid</sub> , BMC, J	0.972	0.970	0.010	0.002
PTH	J	0.927	0.925		<0.001
	J, Ct.Ar <sub>80%L</sub>	0.941	0.938	0.014	0.008
ML+PTH	Ct.Ar <sub>mid</sub>	0.958	0.957		<0.001
	Ct.Ar <sub>mid</sub> , BMC	0.977	0.975	0.019	<0.001
	Ct.Ar <sub>mid</sub> , BMC, Ct.Th	0.981	0.979	0.004	0.011
<b>Stiffness</b>					
OVX	Ct.Ar <sub>mid</sub>	0.503	0.485		<0.001
ML	BMC	0.904	0.901		<0.001
	BMC, J	0.934	0.930	0.030	<0.001

<sup>a</sup>Only models where a significant F-change was found are reported, indicating that additional structural properties improved the predictions of the bone mechanics.

modest, improvements on the prediction of the tibia mechanics (range of the change in  $R^2$ : 0.004–0.030,  $p < 0.01$ , Table 1).

In the “OVX” group, organ level and tissue level properties were modest to good predictors of strength ( $R^2$ -range: 0.652–0.870, all  $p < 0.05$ ), with the exception of Ct.Ar80%L that weakly, albeit significantly, predicted bone strength ( $R^2 = 0.160$ ,  $p = 0.03$ ). Bone structural properties were also poorer predictors of the estimated bone stiffness ( $R^2$ -range: 0.164–0.513, all  $p < 0.05$ ).

The linear regressions for the pooled data from every group are reported in the Supporting Information S1: Figures 5 and 6. They show good to excellent relationships between the densitometric (BMC) and cortical bone properties and the bone stiffness ( $0.770 < R^2 < 0.876$ ) or failure load ( $0.845 < R^2 < 0.942$ ).

The details of the regression coefficients for each group and pooled data are reported in the Supporting Information S1: Tables 4 and 5.

## 4 | DISCUSSION

In this study, we quantified the individual and combined longitudinal effects of PTH(1-34) and mechanical loading on the microFE-derived mechanical properties of mouse tibia in an ovariectomised mouse model of osteoporosis. Combined treatment had increased benefits to the estimated bone stiffness and strength than individual treatments, consistent with greater benefit to structural parameters and confirming the study hypothesis. Both the organ-level and the tissue-level (midshaft) structural properties, including the cortical area and total BMC, were strong predictors of the estimated bone mechanics.

With OVX, the estimated bone stiffness and strength did not change over time, while measures of BMC and the bone morphometric properties were also stable. This result highlights that the OVX model can replicate some of the accelerated bone resorption observed in postmenopausal women with OP but that the reduction of bone mass is not sufficient to reduce the bone strength in mice. This is probably due to the fact that OVX affects mainly the proximal trabecular bone and only at a later stage the cortical bone<sup>18</sup> and that trabecular bone has only a limited influence on the mouse tibia strength.<sup>39</sup> With PTH monotherapy, both the stiffness and strength improved, consistent with findings elsewhere in non-ovariectomised C57BL/6 mice.<sup>25</sup> Mechanical loading similarly improved the tibia mechanics, which to our knowledge had not been quantified longitudinally before. Cross-sectionally, Warden et al.<sup>49</sup> demonstrated the ability for tibia loading to confer structural and strength benefits to the tibia for at least 1 year when ovariectomy induced osteoporosis was performed proceeding the loading bouts. In another cross-sectional study, no or modest significant benefits to the bone axial compressive strength, and unexpectedly a decline in the bone stiffness, were observed,<sup>50</sup> partially in agreement with our findings for loading monotherapy. This discrepancy could in part be attributed to differences in loading regimens across studies or methodological approach comparing *in silico* versus laboratory experiments and longitudinal versus cross-sectional design. In Holguin et al.<sup>50</sup> the loading protocols were defined by a lower load

(10 N), longer treatment duration (6 weeks) and an increased number of daily loading cycles (60 or 1200 cycles/day) than herein, and the authors speculated that the decline in stiffness was a consequence of damage within pre-existing bone, though more deliberate experiments are still required to confirm this hypothesis.

Combining PTH and loading treatments had increased benefits to tibia mechanics (stiffness and strength) and the cortical bone structural properties (BMC, TMD, Ct.Ar, and Ct.Th). The enhanced structural benefits, specifically when combining PTH in the tibia loading model, have been well documented in the C57BL/6 mouse, across either intact, young and aged (19-month-old) or ovariectomised animals and consistent with findings herein.<sup>10,16,22</sup> To our knowledge, the increased benefit to compressive bone mechanics are reported for the first time, though improvements in bending strength has often been inferred from changes in structure for example, an increase in the polar moment of inertia,<sup>22</sup> and according to basic principles of beam theory.<sup>20</sup> This result highlights the potential of combining biomechanical and pharmacological treatments to overcome the effect of accelerated bone resorption induced by decrease in oestrogen in mice, and this option should be considered for future clinical studies. Nevertheless, considering that the external mechanical loading used in this study may induce relatively high deformation in the tibia, combinations of pharmacological treatments with lower strain and strain rate biomechanical intervention (e.g., running on treadmill) should be investigated in the future. It is advantageous of the longitudinal study design that we observe greater osteogenic benefits following the first bout of loading at 19-week-old, at which the largest increase in failure load was also observed (e.g., in ML+PTH change of failure load between Weeks 18 and 20 of age equal to 20% versus change of failure load between Weeks 20 and 22 of age equal to 9%). As the stiffness of the bone increased, we observed that the strains induced by Week 21 loading decreases (Figure 2) and this corresponded with reduced bone formation from 20 to 22 weeks of age.<sup>51,52</sup> As noted in a review by Meakin et al.<sup>36</sup> and more recently Main et al.<sup>35</sup> the peak strain engendered by tibia loading, rather than the magnitude of the applied load, is most important for modulating the bone anabolic response. Thus, the decline in the bone formation rate was not unexpected after the initial loading bout, and an increase in the applied load would be necessary at Week 21 to engender the same response. Future work may consider strain matching across loading bouts, however careful design is emphasized to minimize possible adverse events such as impaired mobility that has been documented in applied loads exceeding 12N.<sup>31</sup>

It is noteworthy that we observed these animals following 2 weeks of treatment withdrawal. Enhanced fracture risk following discontinuation of treatment is of concern.<sup>53</sup> This may be due to poor treatment adherence, or discontinuation as a result of adverse events or following permissible treatment course (e.g., teriparatide treatment is not recommended to exceed 2 years). However, to our knowledge the impact of withdrawal on bone properties has not been observed. We show that benefits in bone mechanics and structure were retained in the 2 weeks following treatment cessation. This could suggest a period exists to transition to alternative therapies without compromise of bone health.

Among all treatment groups the cortical bone organ- and tissue-level structural properties were strong predictors of the estimated tibia stiffness ( $R^2 > 0.724$ ) and strength ( $R^2 > 0.823$ ). This is in contrast with metaphyseal trabecular bone properties which were generally poor predictors of the bone mechanics (Supporting Information; in line with the low contribution of trabecular bone to the structural mechanical properties in the mouse tibia<sup>38</sup>). In comparison, improvements in the trabecular bone mass were strong predictors for increased bone strength of the trabecular rich vertebra where strength was determined per microFE analysis in mice<sup>54</sup> and mechanical testing in humans.<sup>55</sup> The improved ability to predict bone mechanics using the whole tibia versus regional measurements differed among the treatment groups. Generally, in ML and PTH mice, whole tibia properties better predicted stiffness or strength, whereas in ML+PTH, midshaft cortical area better predicted strength than cortical area along the 80%L volume ( $R^2 > 0.85$  in either case). This would suggest that the midshaft morphometric properties are reasonable proxies from which one could infer the bone mechanics, however the biomechanical analyses provide a more detailed assessment of the structural behavior of the bone. As shown in our laboratory and others, whole bone imaging for comprehensive spatial analyses can be critical to elucidate heterogeneous benefits of OP treatments on bone, which could otherwise be underrepresented by standard morphometric analyses at the limb midshaft.<sup>21</sup>

MicroCT imaging is extensively used in preclinical studies to noninvasively measure the bone microstructure and density, and their changes over time.<sup>21,56</sup> Whereas, the therapeutic adaptation of bone mechanics are more commonly evaluated cross-sectionally using destructive mechanical tests.<sup>20</sup> The temporal behavior of bone mechanics is thus evaluated by sacrificing many different groups of mice at different time points, for example,<sup>57,58</sup> Combining the microCT image data with validated microFE models is an important experimental refinement that permits an accurate, noninvasive, and hence longitudinal, estimation of the bone mechanical properties in the targeted limb of the same animal over time. This approach, applied within a longitudinal study design,<sup>59</sup> has contributed to a substantial reduction in the number of animals used herein than is typically used in the preclinical assessment of antiosteoporotic treatment strategies, a fundamental step toward the 3Rs (replacement, refinement, and reduction of the usage of animals in research).<sup>19</sup> Moreover, the longitudinal data has been essential to inform mechanistic models of bone remodeling for example.<sup>51,60,61</sup>

The ovariectomized C57BL/6 mouse is one of the most common models for OP research due to rapid trabecular bone loss in the epiphysis of long bones.<sup>18</sup> Change in cortical bone in the "OVX" group, in which no treatment was provided, was characterized by non-significant and negligible change in cortical bone, which did not translate to a longitudinal change (neither strengthening nor weakening) in the estimated mechanical properties. This is a limitation of this OP model, given that features of the disease include thinning and trabecularization of the cortical bone accompanied by bone weakening. Increased cortical porosity was found in aged (19 month) C57BL/6 mice following sustained (4–6 weeks) administration of PTH(1-34),<sup>10</sup> but not

over a 2-week treatment period and as confirmed by the work in younger, ovariectomized mice herein. Certainly, there is work to identify more relevant bone sites to the human disease, for example, at the femoral neck.<sup>62</sup> However, study of the femur or vertebra in mice present their own disadvantages. For example, these anatomical sites present differently than in primates, the loading conditions can be difficult to control, and imaging (excluding caudal vertebra) is not possible in vivo without exposing large ionizing radiation dose to vital organs. While we acknowledge that the model may only represent some of the phenotypes of OP, it was useful to demonstrate benefits in all treatments (pharmacological, biomechanical, and combined) with oestrogen deficiency.

## 4.1 | Limitations

There were limitations in our study. First, in the in vivo study we have not included a sham operated group as control to evaluate the effect of ovariectomy on the mechanical properties of the mouse tibia. In two previous studies we have found (1) no significant differences in densitometric properties of the mouse tibia between sham operated and non-operated C57BL/6 mice (unpublished data) and (2) significant differences between the morphometric and densitometric properties of the mouse tibia of ovariectomized and non-operated C57BL/6 mice, which however did not affect the tibia mechanical properties estimated with microFE models.<sup>18</sup> This result could be due to the fact that ovariectomy affects mainly the trabecular bone, which in the mouse tibia is found mainly in the most proximal portion of the bone. It remains to be investigated what would be the effect of combined treatments on sham operated mice. Therefore, as mentioned above, while ovariectomy is considered the best model of osteoporosis in rodents, further studies should be performed in this area to understand its validity when testing the effect of new treatments on the bone mechanical properties. Second, the in vivo study design precludes microCT scanning at smaller voxel size without increased radiation dose. PTH, depending on the dosing strategy, is shown to increase the cortical bone porosity, including in 19-month-old C57BL/6 mice.<sup>10</sup> The intracortical pores may only be  $<10\ \mu\text{m}$  in diameter.<sup>63</sup> Thus, we could not reasonably resolve these features in our images and pores were not incorporated in our microFE models, though elsewhere increased porosity has been associated with increased bone fragility.<sup>63,64</sup> Regardless, we report good agreement between experimental and predicted bone mechanics from recent validation experiments within our group, and that included left tibiae of the ovariectomized and PTH-treated mouse reported herein.<sup>23</sup> Third, linear homogeneous microFE models were used. Assigning heterogeneous material properties to the microFE models could, in part, account for heterogeneity in local mineralization of the bone. While bone stiffness predictions were not improved in our microFE model validation study as the model complexity was increased,<sup>23</sup> it remains to be investigated if heterogeneous models would improve the predictions of tibia mechanical properties remodeled due to controlled, externally applied loading. Similarly, nonlinear models

could be implemented to account for local damage and localization of deformation in tibia from OVX and treated bones. Nonlinear microFE models have been recently applied to the human radius from lower resolution images<sup>65</sup> and future applications in preclinical studies to evaluate the bone strength in the mouse tibia could be explored, after proper validation versus experiments and improvement of microFE model efficiency.

## 5 | CONCLUSION

Combining PTH(1-34) and tibia loading had increased benefits to the tibia bone stiffness and strength than individual therapies. The bone mechanics were strongly related to both the bone organ-level and tissue-level structural properties that similarly improved with treatment. Our longitudinal data shows that the mono- and combined therapies had continued benefit (i.e., a persistent increase) to bone structure and strength over time. Furthermore, that these benefits were retained after withdrawal of treatment. This data highlights the utility of microCT informed microFE models to quantify bone mechanics in preclinical imaging studies for testing novel treatments of low bone mass in osteoporosis.

## AUTHOR CONTRIBUTIONS

Bryant C. Roberts contributed to research design, the acquisition, analysis and interpretation of data and drafting and revision of the manuscript. Vee San Cheong, Sara Oliviero, Hector M. Arredondo Carrera, and Ning Wang contributed to the acquisition and interpretation of data and critical revision of the manuscript. Alison Gartland was involved in interpretation of the data and critical revision of the manuscript. Enrico Dall'Ara contributed to research design, the analysis and interpretation of data and drafting and revision of the manuscript. All authors contributed to and approved the final article for submission.

## ACKNOWLEDGMENTS

This study was funded by the EPSRC Frontier Engineering Awards, MultiSim and MultiSim2 projects (Grant Reference Numbers: EP/K03877X/1 and EP/S032940/1) and the UK National Centre for the Replacement, Refinement and Reduction of Animals in Research (NC3Rs, grant number: NC/R001073/1). The authors thank Sahand Zanjani-pour, Maya Boudiffa, Matthew Fisher, Svetlana Soloviena, and Richard Allen for technical assistance and The University of Sheffield Skeletal laboratory (<http://skeletal.group.shef.ac.uk>) for access to the scanning facilities.

## ORCID

Enrico Dall'Ara  <http://orcid.org/0000-0003-1471-5077>

## REFERENCES

1. Johnell O, Kanis JA. An estimate of the worldwide prevalence and disability associated with osteoporotic fractures. *Osteoporos Int*. 2006;17:1726-1733.
2. Kanis JA, Glüer C-C. An update on the diagnosis and assessment of osteoporosis with densitometry. *Osteoporos Int*. 2000;11:192-202.
3. Cummings SR, Cosman F, Eastell R, Reid IR, Mehta M, Lewiecki EM. Goal-directed treatment of osteoporosis. *J Bone Miner Res*. 2013;28:433-438.
4. Graeff C, Chevalier Y, Charlebois M, et al. Improvements in vertebral body strength under teriparatide treatment assessed in vivo by finite element analysis: results from the EUROFOR study. *J Bone Miner Res*. 2009;24:1672-1680.
5. Keaveny TM, Hoffmann PF, Singh M, et al. Femoral bone strength and its relation to cortical and trabecular changes after treatment with PTH, alendronate, and their combination as assessed by finite element analysis of quantitative CT scans. *J Bone Miner Res*. 2008;23:1974-1982.
6. Bouxsein ML, Eastell R, Lui L-Y, et al. Change in bone density and reduction in fracture risk: a meta-regression of published trials. *J Bone Miner Res*. 2019;34:632-642.
7. Appelman-Dijkstra NM, Oei H, Vlug AG, Winter EM. The effect of osteoporosis treatment on bone mass. *Best Pract Res Clin Endocrinol Metab*. 2022;36:101623.
8. Neer RM, Arnaud CD, Zanchetta JR, et al. Effect of parathyroid hormone (1-34) on fractures and bone mineral density in postmenopausal women with osteoporosis. *N Engl J Med*. 2001;344:1434-1441.
9. Fink HA, MacDonald R, Forte ML, et al. Long-term drug therapy and drug discontinuations and holidays for osteoporosis fracture prevention: a systematic review. *Ann Intern Med*. 2019;171:37-50.
10. Meakin LB, Todd H, Delisser PJ, et al. Parathyroid hormone's enhancement of bones' osteogenic response to loading is affected by ageing in a dose- and time-dependent manner. *Bone*. 2017;98:59-67.
11. Haas AV, LeBoff MS. Osteoanabolic agents for osteoporosis. *J Endocr Soc*. 2018;2:922-932.
12. Vandamme T. Use of rodents as models of human diseases. *J Pharm BioAllied Sci*. 2014;6:2-9.
13. Perilli E, Le V, Ma B, Salmon P, Reynolds K, Fazzalari NL. Detecting early bone changes using in vivo micro-CT in ovariectomized, zoledronic acid-treated, and sham-operated rats. *Osteoporos Int*. 2010;21:1371-1382.
14. Brouwers JEM, van Rietbergen B, Huiskes R, Ito K. Effects of PTH treatment on tibial bone of ovariectomized rats assessed by in vivo micro-CT. *Osteoporos Int*. 2009;20:1823-1835.
15. Ko C-Y, Jung YJ, Park JH, et al. Trabecular bone response to mechanical loading in ovariectomized Sprague-Dawley rats depends on baseline bone quantity. *J Biomech*. 2012;45:2046-2049.
16. Roberts BC, Arredondo Carrera HM, Zanjani-pour S, et al. PTH (1-34) treatment and/or mechanical loading have different osteogenic effects on the trabecular and cortical bone in the ovariectomized C57BL/6 mouse. *Sci Rep*. 2020;10:8889.
17. Klinck J, Boyd SK. The magnitude and rate of bone loss in ovariectomized mice differs among inbred strains as determined by longitudinal in vivo micro-computed tomography. *Calcif Tissue Int*. 2008;83:70-79.
18. Roberts BC, Giorgi M, Oliviero S, Wang N, Boudiffa M, Dall'Ara E. The longitudinal effects of ovariectomy on the morphometric, densitometric and mechanical properties in the murine tibia: a comparison between two mouse strains. *Bone*. 2019;127:260-270.
19. Viceconti M, Dall'Ara E. From bed to bench: how in silico medicine can help ageing research. *Mech Ageing Dev*. 2019;177:103-108.
20. Jepsen KJ, Silva MJ, Vashishth D, Guo XE, van der Meulen MC. Establishing biomechanical mechanisms in mouse models: practical guidelines for systematically evaluating phenotypic changes in the diaphyses of long bones. *J Bone Miner Res*. 2015;30:951-966.
21. Bouxsein ML, Boyd SK, Christiansen BA, Guldberg RE, Jepsen KJ, Müller R. Guidelines for assessment of bone microstructure in



- rodents using micro-computed tomography. *J Bone Miner Res.* 2010;25:1468-1486.
22. Sugiyama T, Saxon LK, Zaman G, et al. Mechanical loading enhances the anabolic effects of intermittent parathyroid hormone (1-34) on trabecular and cortical bone in mice. *Bone.* 2008;43:238-248.
23. Oliviero S, Roberts M, Owen R, Reilly GC, Bellantuono I, Dall'Ara E. Non-invasive prediction of the mouse tibia mechanical properties from microCT images: comparison between different finite element models. *Biomech Model Mechanobiol.* 2021;20:941-955.
24. Oliviero S, Owen R, Reilly GC, Bellantuono I, Dall'Ara E. Optimization of the failure criterion in micro-finite element models of the mouse tibia for the non-invasive prediction of its failure load in preclinical applications. *J Mech Behav Biomed Mater.* 2021;113:104190.
25. Lu Y, Boudiffa M, Dall'Ara E, Liu Y, Bellantuono I, Viceconti M. Longitudinal effects of parathyroid hormone treatment on morphological, densitometric and mechanical properties of mouse tibia. *J Mech Behav Biomed Mater.* 2017;75:244-251.
26. Alexander JM, Bab I, Fish S, et al. Human parathyroid hormone 1-34 reverses bone loss in ovariectomized mice. *J Bone Miner Res.* 2001;16:1665-1673.
27. Monzem S, Valkani D, Evans LAE, Chang YM, Pitsillides AA. Regional modular responses in different bone compartments to the anabolic effect of PTH (1-34) and axial loading in mice. *Bone.* 2023;170:116720.
28. Glatt V, Canalis E, Stadmeier L, Bouxsein ML. Age-related changes in trabecular architecture differ in female and male C57BL/6J mice. *J Bone Miner Res.* 2007;22:1197-1207.
29. Kramer I, Loots GG, Studer A, Keller H, Kneissel M. Parathyroid hormone (PTH)-induced bone gain is blunted in SOST overexpressing and deficient mice. *J Bone Miner Res.* 2010;25:178-189.
30. Zweifler LE, Koh AJ, Daignault-Newton S, McCauley LK. Anabolic actions of PTH in murine models: two decades of insights. *J Bone Miner Res.* 2021;36:1979-1998.
31. De Souza RL, Matsuura M, Eckstein F, Rawlinson SCF, Lanyon LE, Pitsillides AA. Non-invasive axial loading of mouse tibiae increases cortical bone formation and modifies trabecular organization: a new model to study cortical and cancellous compartments in a single loaded element. *Bone.* 2005;37:810-818.
32. Oliviero S, Giorgi M, Dall'Ara E. Validation of finite element models of the mouse tibia using digital volume correlation. *J Mech Behav Biomed Mater.* 2018;86:172-184.
33. Giorgi M, Dall'Ara E. Variability in strain distribution in the mice tibia loading model: a preliminary study using digital volume correlation. *Med Eng Phys.* 2018;62:7-16.
34. Srinivasan S, Weimer DA, Agans SC, Bain SD, Gross TS. Low-magnitude mechanical loading becomes osteogenic when rest is inserted between each load cycle. *J Bone Miner Res.* 2002;17:1613-1620.
35. Main RP, Shefelbine SJ, Meakin LB, Silva MJ, van der Meulen MCH, Willie BM. Murine axial compression tibial loading model to study bone mechanobiology: implementing the model and reporting results. *J Orthop Res.* 2020;38:233-252.
36. Meakin LB, Price JS, Lanyon LE. The contribution of experimental in vivo models to understanding the mechanisms of adaptation to mechanical loading in bone. *Front Endocrinol.* 2014;5:154.
37. Sun D, Brodt MD, Zannit HM, Holguin N, Silva MJ. Evaluation of loading parameters for murine axial tibial loading: stimulating cortical bone formation while reducing loading duration. *J Orthop Res.* 2018;36:682-691.
38. Oliviero S, Lu Y, Viceconti M, Dall'Ara E. Effect of integration time on the morphometric, densitometric and mechanical properties of the mouse tibia. *J Biomech.* 2017;65:203-211.
39. Oliviero S, Giorgi M, Laud PJ, Dall'Ara E. Effect of repeated in vivo microCT imaging on the properties of the mouse tibia. *PLoS ONE.* 2019;14:e0225127.
40. Kazakia GJ, Burghardt AJ, Cheung S, Majumdar S. Assessment of bone tissue mineralization by conventional x-ray microcomputed tomography: comparison with synchrotron radiation microcomputed tomography and ash measurements. *Med Phys.* 2008;35:3170-3179.
41. Campbell GM, Tiwari S, Grundmann F, Purcz N, Schem C, Glüer CC. Three-dimensional image registration improves the long-term precision of in vivo micro-computed tomographic measurements in anabolic and catabolic mouse models. *Calcif Tissue Int.* 2014;94:282-292.
42. Christiansen BA. Effect of micro-computed tomography voxel size and segmentation method on trabecular bone microstructure measures in mice. *Bone Rep.* 2016;5:136-140.
43. Oliviero S, Millard E, Chen Z, et al. Accuracy of in vivo microCT imaging in assessing the microstructural properties of the mouse tibia subchondral bone. *Front Endocrinol.* 2023;13:1016321.
44. Lu Y, Boudiffa M, Dall'Ara E, Bellantuono I, Viceconti M. Development of a protocol to quantify local bone adaptation over space and time: quantification of reproducibility. *J Biomech.* 2016;49:2095-2099.
45. Salmon PL, Monzem S, Javaheri B, Oste L, Kerckhofs G, Pitsillides AA. Resolving trabecular metaphyseal bone profiles downstream of the growth plate adds value to bone histomorphometry in mouse models. *Front Endocrinol.* 2023;14:839.
46. Galea GL, Hannuna S, Meakin LB, Delisser PJ, Lanyon LE, Price JS. Quantification of alterations in cortical bone geometry using site specificity software in mouse models of aging and the responses to ovariectomy and altered loading. *Front Endocrinol.* 2015;6:52.
47. Meng X, Rosenthal R, Rubin DB. Comparing correlated correlation coefficients. *Psychol Bull.* 1992;111:172-175.
48. Yang H, Butz KD, Duffy D, Niebur GL, Nauman EA, Main RP. Characterization of cancellous and cortical bone strain in the in vivo mouse tibial loading model using microCT-based finite element analysis. *Bone.* 2014;66:131-139.
49. Warden SJ, Galley MR, Hurd AL, et al. Cortical and trabecular bone benefits of mechanical loading are maintained long term in mice independent of ovariectomy. *J Bone Miner Res.* 2014;29:1131-1140.
50. Holguin N, Brodt MD, Sanchez ME, Kotiya AA, Silva MJ. Adaptation of tibial structure and strength to axial compression depends on loading history in both C57BL/6 and BALB/c mice. *Calcif Tissue Int.* 2013;93:211-221.
51. Cheong VS, Roberts BC, Kadirkamanathan V, Dall'Ara E. Bone remodelling in the mouse tibia is spatio-temporally modulated by oestrogen deficiency and external mechanical loading: a combined in vivo/in silico study. *Acta Biomater.* 2020;116:302-317.
52. Cheong VS, Roberts BC, Kadirkamanathan V, Dall'Ara E. Positive interactions of mechanical loading and PTH treatments on spatio-temporal bone remodelling. *Acta Biomater.* 2021;136:291-305.
53. Langdahl BL, Silverman S, Fujiwara S, et al. Real-world effectiveness of teriparatide on fracture reduction in patients with osteoporosis and comorbidities or risk factors for fractures: integrated analysis of 4 prospective observational studies. *Bone.* 2018;116:58-66.
54. Lambers FM, Schulte FA, Kuhn G, Webster DJ, Müller R. Mouse tail vertebrae adapt to cyclic mechanical loading by increasing bone formation rate and decreasing bone resorption rate as shown by time-lapsed in vivo imaging of dynamic bone morphometry. *Bone.* 2011;49:1340-1350.
55. Perilli E, Briggs AM, Kantor S, et al. Failure strength of human vertebrae: prediction using bone mineral density measured by DXA and bone volume by micro-CT. *Bone.* 2012;50:1416-1425.
56. van't Hof RJ, Dall'Ara E. Analysis of bone architecture in rodents using micro-computed tomography. In: Idris AI, ed. *Bone Research Protocols.* Springer New York; 2019:507-531.
57. Deckard C, Walker A, Hill BJF. Using three-point bending to evaluate tibia bone strength in ovariectomized young mice. *J Biol Phys.* 2017;43:139-148.



58. Mumtaz H, Dallas M, Begonia M, et al. Age-related and sex-specific effects on architectural properties and biomechanical response of the C57BL/6N mouse femur, tibia and ulna. *Bone Rep.* 2020;12:100266.
59. Dall'Ara E, Boudiffa M, Taylor C, et al. Longitudinal imaging of the ageing mouse. *Mech Ageing Dev.* 2016;160:93-116.
60. Cheong VS, Campos Marin A, Lacroix D, et al. A novel algorithm to predict bone changes in the mouse tibia properties under physiological conditions. *Biomech Model Mechanobiol.* 2019;19:985-1001.
61. Cheong VS, Kadiramanathan V, Dall'Ara E. The role of the loading condition in predictions of bone adaptation in a mouse tibial loading model. *Front Bioeng Biotechnol.* 2021;9:676867.
62. Monzem S, Gohin S, YagüeBallester R, Lopes de Souza R, Meeson R, Pitsillides AA. An examination of two different approaches for the study of femoral neck fracture: towards a more relevant rodent model. *Proc Inst Mech Eng Part H.* 2022;236:199-207.
63. Schneider P, Voide R, Stampanoni M, Donahue LR, Müller R. The importance of the intracortical canal network for murine bone mechanics. *Bone.* 2013;53:120-128.
64. Carriero A, Doube M, Vogt M, et al. Altered lacunar and vascular porosity in osteogenesis imperfecta mouse bone as revealed by synchrotron tomography contributes to bone fragility. *Bone.* 2014;61:116-124.
65. Stipsitz M, Zysset PK, Pahr DH. Prediction of the inelastic behaviour of radius segments: damage-based nonlinear micro finite element simulation vs Pistoia criterion. *J Biomech.* 2021;116:110205.

## SUPPORTING INFORMATION

Additional supporting information can be found online in the Supporting Information section at the end of this article.

**How to cite this article:** Roberts BC, Cheong VS, Oliviero S, et al. Combining PTH(1-34) and mechanical loading has increased benefit to tibia bone mechanics in ovariectomised mice. *J Orthop Res.* 2024;1-13. doi:10.1002/jor.25777